

Research Article

Identification of a core set of genes that signifies pathways underlying cardiac hypertrophy

Claes C. Strøm¹, Mogens Kruhøffer², Steen Knudsen³, Frank Stensgaard-Hansen¹, Thomas E. N. Jonassen⁴, Torben F. Ørntoft², Stig Haunsø¹ and Søren P. Sheikh¹*

¹CHARC (Copenhagen Heart Arrhythmia Research Center), Department of Medicine B, H:S Rigshospitalet, University of Copenhagen Medical School, 2100 Copenhagen, Denmark

²Molecular Diagnostic Laboratory, Department of Clinical Biochemistry, Aarhus University Hospital, Denmark

³Center for Biological Sequence Analysis, Technical University of Denmark, 2800 Kgs. Lyngby, Denmark

⁴Department of Pharmacology, Copenhagen University, 2100 Copenhagen, Denmark

*Correspondence to:

Søren P. Sheikh, Lab. Mol. Card.,
Department of Medicine B, H:S
Rigshospitalet, University of
Copenhagen, 20 Juliane
Mariesvej, DK-2100
Copenhagen, Denmark.
E-mail: sheikh@molheart.dk

Abstract

Although the molecular signals underlying cardiac hypertrophy have been the subject of intense investigation, the extent of common and distinct gene regulation between different forms of cardiac hypertrophy remains unclear. We hypothesized that a general and comparative analysis of hypertrophic gene expression, using microarray technology in multiple models of cardiac hypertrophy, including aortic banding, myocardial infarction, an arteriovenous shunt and pharmacologically induced hypertrophy, would uncover networks of conserved hypertrophy-specific genes and identify novel genes involved in hypertrophic signalling. From gene expression analyses (8740 probe sets, $n = 46$) of rat ventricular RNA, we identified a core set of 139 genes with consistent differential expression in all hypertrophy models as compared to their controls, including 78 genes not previously associated with hypertrophy and 61 genes whose altered expression had previously been reported. We identified a single common gene program underlying hypertrophic remodelling, regardless of how the hypertrophy was induced. These genes constitute the molecular basis for the existence of one main form of cardiac hypertrophy and may be useful for prediction of a common therapeutic approach. Supplementary material for this article can be found at: <http://www.interscience.wiley.com/jpages/1531-6912/suppmat>
Copyright © 2004 John Wiley & Sons, Ltd.

Received: 6 February 2004
Revised: 30 August 2004
Accepted: 21 September 2004

Keywords: cardiac hypertrophy; remodelling; gene expression; DNA microarrays

Introduction

Cardiac hypertrophy is a compensatory mechanism to augment cardiac output after biomechanical stress. Sustained hypertrophy leads to cardiac dysfunction, heart failure and arrhythmia, hence hypertrophy is an independent risk factor for cardiac morbidity and mortality (Agabiti-Rosei *et al.*, 1997). Understanding the genes that govern cardiomyocyte hypertrophic properties has implications for both clinical medicine and basic cell biology.

Cardiac hypertrophy appears in different phenotypes, depending on the eliciting stimuli; however, it is unclear whether this is the result of divergent transcriptional responses or if a common hypertrophy gene program exists (Aronow *et al.*, 2001; Chien *et al.*, 1991; Wollert *et al.*, 1996). The structural changes in the left ventricle including eccentric and concentric hypertrophy can be mimicked in animal models by volume and pressure overload procedures, respectively. Eccentric hypertrophy is characterized by left ventricular dilation

and decreased wall thickness, while in concentric hypertrophy the ventricular wall is thickened and the left ventricle reduced. Typically, arteriovenous shunts and myocardial infarction induce eccentric hypertrophy, while aortic banding elicits the concentric phenotype.

Multiple genes change expression in cardiac hypertrophy including genes involved in metabolism, cell growth, apoptosis, cytoskeletal and extracellular matrix (ecm) organization, signal transduction and cell defence (Anversa *et al.*, 1983; Barrans *et al.*, 2002; Friddle *et al.*, 2000; Hwang *et al.*, 2000, 2002; Schoenfeld *et al.*, 1998; Sehl *et al.*, 2000; Stanton *et al.*, 2000; Yang *et al.*, 2000). Several genes are bona fide molecular markers for hypertrophy, including immediate early genes, ANP, BNP, and myosin heavy and light chain isoforms.

However, a comprehensive analysis and direct comparison of the expression changes in different forms of cardiac hypertrophy is lacking. Such an approach may identify shared molecular networks in hypertrophy and point to new therapeutic strategies that interrupt the underlying disease pathways. DNA microarrays allow simultaneous analysis of thousands of genes, and have been useful in analysis of cellular responses to different stimuli, animal models of human disease and cancer classification (Golub *et al.*, 1999; Roberts *et al.*, 2000). Using this technology, we attempted to define a unified gene response that characterizes cardiac hypertrophy by comparing transcriptional profiles from multiple models, including aortic banding, myocardial infarction, arteriovenous shunting and pharmacologically induced hypertrophy. Our results provide a detailed view of the shared gene expression patterns in different hypertrophic phenotypes. Out of 8740 analysed genes on 46 microarrays, we identified a set of 139 genes with common regulation in all hypertrophy models, supporting the notion of a common hypertrophic gene program.

Methods

Cardiac hypertrophy models

Male Wistar rats were used in all experiments. All operations were performed during anaesthesia with fentanyl/fluanisone and midazolam. The investigation conforms to the *Guide for the Care and Use of*

Laboratory Animals, published by the US National Institutes of Health (NIH Publication No. 85-23, revised 1996). Animals were subjected to echocardiographic examination under isoflurane anaesthesia before being sacrificed. Thereafter, the hearts were excised, rinsed in ice-cold saline, weighed, dissected into left and right ventricles, frozen in liquid nitrogen and stored at -80°C before mRNA extraction.

Neonatal hearts were harvested 3 days postpartum.

Aortic banding (AB)

A titanium clip with an inner diameter of 0.6 mm was placed around the ascending aorta, using a custom-made applicator (Weck Closure Systems, USA). Control animals underwent the same procedure except for placement of the clip. The animals were sacrificed after 6, 12, 16 or 30 weeks.

Myocardial infarction (MI)

The LAD coronary artery was occluded with a 6-0 silk ligature immediately below the left atrial appendage. In sham-operated animals, the ligature was passed under the artery and removed. Animals were sacrificed 3 or 9 weeks after surgery. Only hearts with large transmural infarctions were considered for microarray analysis. The scar tissue was removed and discarded.

Aorto-caval fistula (shunt)

The aorta was punctured caudal to the left renal artery with an 18-gauge needle that was subsequently advanced into the vena cava. The needle was withdrawn and the aortic puncture point was sealed with cyanoacrylate glue. The patency of the shunt was verified visually before closure. Control animals underwent the same procedure except for puncture of the vessels. The animals were sacrificed after 3 or 8 weeks.

Hormone treatment

Angiotensin II (AngII; 200 ng/kg/min) was administered subcutaneously for 2 weeks, using implanted miniosmotic pumps (ALZET[®], USA). AngII was diluted in 0.9% NaCl with 0.01 M acetic acid. Age-matched control animals received pumps containing vehicle only. The thyroxin analogue

3,5-diiodothyropropionic acid (Ditpa) was administered as daily subcutaneous injections of 1000 mg/kg. Controls were given saline.

Echocardiography

Echocardiography was performed during anaesthesia with 1–1.5% isoflurane using a Vivid Five Echocardiograph from GE Medical Systems Ultrasound. Recordings were stored digitally for off-line analysis. Left ventricular cavity and wall dimensions were measured in 2D short axis recordings.

Gene expression profiling

GeneChip RGU34A from Affymetrix containing 8740 genes (and 59 control genes, which were excluded from further analysis) was used for all hybridizations. Approximately 6000 known genes are represented on the chip, the rest being ESTs (see www.affymetrix.com for a more detailed description). Standard protocols for chip hybridizations were used. At each time point in each model, both diseased and control animals were randomly split into two to four groups, and RNA isolated from the left ventricle from animals in each group were pooled and hybridized to the oligonucleotide arrays. Thus, each time point in each model is represented by four to six (two to four diseased, and two controls) independent RNA pools, each hybridized to an array, in total 46 arrays. Raw data are available at www.ncbi.nlm.nih.gov/geo as Series No. GSE 738.

Array data analysis

Array data were normalized using the non-linear invariant rank fitting method of Li and Wong, available at www.dchip.org (Li *et al.*, 2001a, 2001b). Model-based expression values (MBE) were calculated for each gene using dChip (perfect match only model). For each hypertrophic sample, a log fold change was calculated for each gene by dividing the MBE value by the average MBE value of the two relevant control samples and then applying \log_2 . This approach was taken to minimize variance not related to hypertrophy between samples.

Statistical significance

Genes with common regulation in different hypertrophic samples were identified using Wilcoxon's

rank sum test on the log fold changes, while ANOVA was used to identify differences between the models. The *p* values calculated for each gene were Bonferroni corrected by discarding all genes with a *p* value higher than 0.05 divided by the number of genes. The Bonferroni correction is a method to control type 1 error when doing multiple comparisons. The principle is to divide the desired type 1 error (usually 0.05) by the number of comparisons.

Clustering

For calculation of distances between genes, fold change was calculated by divided individual MBE by the average MBE of all control samples and applying \log_2 . Vector angle distance on means normalized data is identical to the Pearson correlation. So the only difference between Pearson correlation and vector angle is a normalization step. Hierarchical clustering was applied (weighted pair-group average linkage) and visualized using ClustArray (C. Workman, unpublished; www.cbs.dtu.dk).

Real-time PCR

cDNA was synthesized from single samples previously analysed on GeneChips. Reverse transcription was performed using Superscript II RT (Invitrogen). 1 μ g total RNA and 1 μ l 50 pmol/ μ l (dT)₂₄-primer in a total volume of 12 μ l was incubated for 10 min at 70 °C and chilled on ice. After adding 4 μ l 1st Strand Buffer (from supplier), 1 μ l DTT (0.1 M), 2 μ l dNTP mix (10 mM) and 1 μ l SuperScript RT II (200 U/ μ l), the reaction was incubated for 1 h at 42 °C and finally for 5 min at 95 °C. The cDNA was diluted 1:20 for use in real-time PCR. Real-time PCR analysis was performed on selected genes using the primers shown in Figure 1. Primers were designed using the Primer3 software available at www-genome.wi.mit.edu/cgi-bin/primer/primer3-www.cgi. Triple determinations were performed on the ABI PRISM[®] 7000 Sequence Detection System using the SYBR[®] Green PCR Master Mix (Applied Biosystems, USA). To determine the relative gene expression, a standard curve was made with serial dilutions of a reference sample. The gene expression in the sample of interest was then determined relative to the expression in the reference sample via the standard curve (built-in feature of the analysis software, ABI

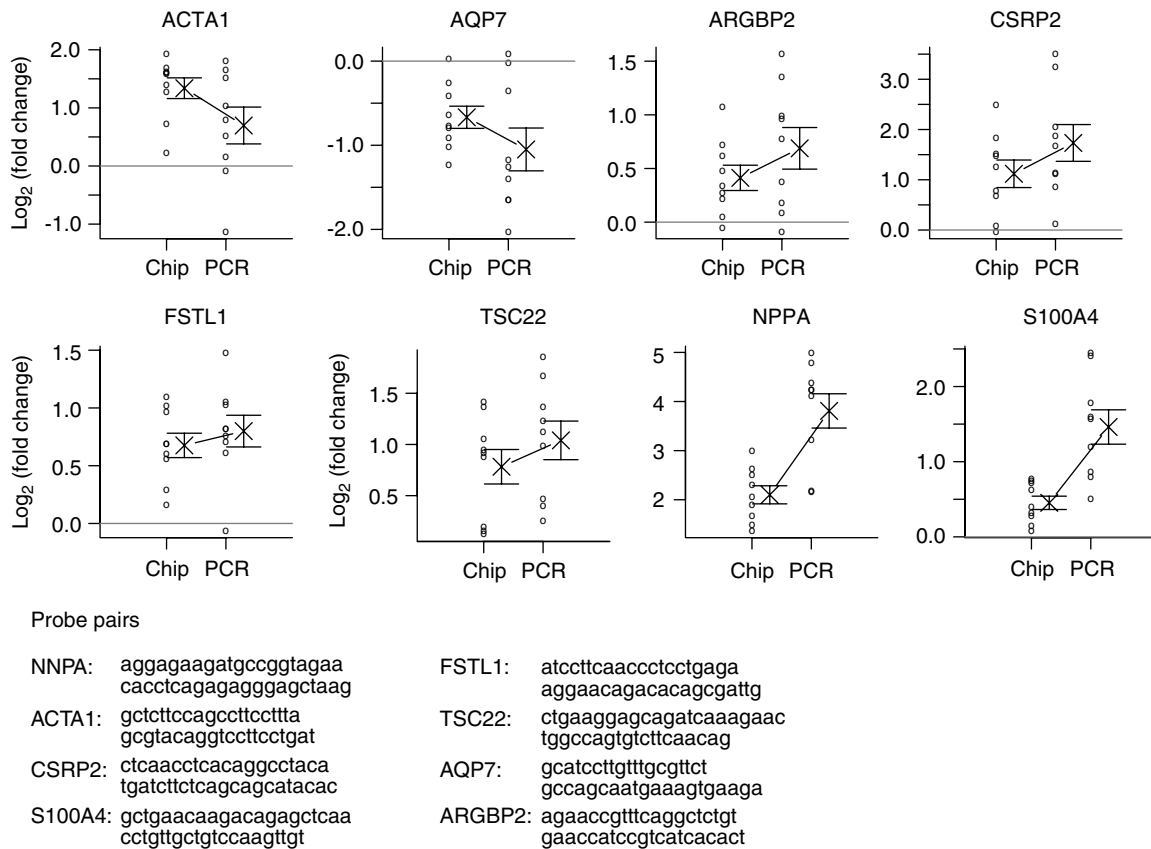


Figure 1. Expression of selected genes was confirmed by real-time PCR. The fold changes of individual genes were calculated as the \log_2 ratio of expression values between hypertrophic samples and their controls. Individual data points are represented by open circles and no change in expression is indicated by grey lines. Means are shown by a cross and SEM by arrows

Prism 7000 SDS Software 1.0.1). The PCR reaction consisted of 12.5 μ l SYBR Green PCR Master Mix, 300 nM forward and reverse primers, and 2.5 μ l 1:20 diluted template cDNA in a total volume of 25 μ l. The reaction was thermocycled using the default settings of ABI Prism 7000 SDS Software 1.0.1: 2 min at 50°C, 10 min at 95°C, followed by 40 rounds of 15 s at 95°C and 1 min at 60°C. A dissociation protocol was added after thermocycling, determining dissociation of the PCR products from 65°C to 95°C. All samples were normalized to GAPDH. For each sample a triple determination was made for each gene of interest and the normalization gene (GAPDH). An average was calculated for the triple determinations. To normalize the gene expression for a specific sample, the average expression value was divided by the average expression value for the normalization gene in the

same sample. According to the GeneChip data, GAPDH is consistently expressed in our samples. Signals from GeneChip analyses were compared to the normalized real-time PCR data.

Results

Animal models for cardiac hypertrophy

All experimental models of cardiac hypertrophy resulted in significant left ventricular hypertrophy (Table 1). In animals with a myocardial infarction (MI), echocardiographic examination revealed massive dilation of the left ventricular cavity, thinning of the anterior wall due to infarction, and decreased systolic function (Table 2). Pressure overload induced by aortic banding (AB) resulted

Table 1. Heart weights

	Weeks	n	HWMI	LVMI
Aortic banding	6	6	5.0 ± 0.16*	3.7 ± 0.14*
Sham	6	6	3.0 ± 0.06	2.0 ± 0.04
Aortic banding	12	6	4.0 ± 0.26*	2.9 ± 0.17*
Sham	12	6	2.5 ± 0.04	1.7 ± 0.01
Aortic banding	16	8	4.3 ± 0.17*	3.0 ± 0.08*
Sham	16	6	2.6 ± 0.07	1.7 ± 0.03
Aortic banding	30	8	4.3 ± 0.37*	2.9 ± 0.20*
Sham	30	6	2.3 ± 0.09	1.5 ± 0.06
MI	3	19	3.7 ± 0.10*	2.2 ± 0.05*
Sham	3	6	3.0 ± 0.06	1.9 ± 0.04
MI	9	14	3.5 ± 0.12*	2.1 ± 0.04*
Sham	9	6	2.6 ± 0.07	1.7 ± 0.04
Shunt	3	10	4.0 ± 0.19*	2.5 ± 0.08*
Sham	3	6	2.8 ± 0.05	1.9 ± 0.03
Shunt	8	12	4.0 ± 0.23*	2.5 ± 0.11*
Sham	8	6	2.7 ± 0.07	1.8 ± 0.04
Angiotensin II	2	12	3.1 ± 0.04*	2.1 ± 0.05*
Ditpa	2	11	3.2 ± 0.1*	2.2 ± 0.10*
Vehicle	2	21	2.8 ± 0.04	1.9 ± 0.03

Values are listed as mean ± SEM. Heart weights (HW) and left ventricular (LV) weights were divided by body weights (HWMI and LVMI). Other abbreviations used: 3,5-diiodothyropropionic acid (Ditpa), myocardial infarction (mi), * $p < 0.05$ vs. sham/vehicle.

in wall thickening but no dilation of the left ventricular cavity consistent with concentric hypertrophy. Systolic function was preserved in these animals. Volume overload induced by a shunt between the aorta and the caval vein was characterized by ventricular dilation and no or marginal increases in wall thickness consistent with eccentric hypertrophy. Systolic function was marginally depressed in the volume-overloaded animals.

A unified gene expression response to cardiac hypertrophy

To identify genes with a common gene expression pattern in hypertrophy, we analysed cardiac gene expression by DNA microarrays. After normalization to the appropriate controls, consistent gene expression changes between the different phenotypes of cardiac hypertrophy were identified by comparing gene expression changes in the different models using a Wilcoxon test. To avoid false positives as a result of multiple testing, p values were Bonferroni-corrected, such that the risk of one or more false positive results was less than 5%.

This procedure identified 179 genes, representing 139 known genes, 13 ESTs and 27 gene duplicates that were significantly regulated in hypertrophic

hearts vs. controls (Table 3 in this paper, and Supplemental Table A). Among the 179 genes, 137 were upregulated and 42 downregulated. Of the 139 known genes, 61 have previously been reported to change expression in response to hypertrophy, while 78 have not previously been connected with hypertrophy. A literature search revealed that 30 of the 137 genes have previously been reported to change at the protein level (Supplemental Table A). This confirms that many of the transcriptome changes actually result in changed cellular protein, considering that only 61 genes had previously been associated with hypertrophy.

Figure 2 depicts a hierarchic cluster analysis of the commonly regulated genes. All duplicate genes were equally regulated and clustered tightly together. The genes fell into two major clusters, representing up- and downregulated genes, respectively.

Classification into seven major categories based on biological function revealed that the core hypertrophy-related genes were predominantly involved in metabolism, signal transduction, cytoskeletal/ecm organization, and cell defence/inflammation (Figure 3). Most notably, in the cluster of downregulated genes (Figure 2) the vast majority of genes were involved in β -oxidation of fatty acids and oxidative phosphorylation.

Cardiac hypertrophy is associated with extensive remodelling of the extracellular matrix. In line with this notion, we observed enhanced expression of several ecm genes previously associated with hypertrophy (fibronectin, vimentin, biglycan, tissue-inhibitor of metalloproteinase-1 and -2, and osteopontin) and genes not previously connected with myocardial remodelling (protease nexin-1, profilin-1 and osteoprotegerin). Several cytoskeletal genes were also upregulated (skeletal and vascular smooth muscle α -actin). Several genes involved in inflammation were upregulated (Hsp27, Psme1, Pai1, and several complement genes), confirming the notion that inflammation is important in the hypertrophic process.

Genes involved in cell growth and proliferation included cyclin D2, FSTL1 and S100A4, confirming previous observations that cyclin D2 protein is upregulated in aortic-banded rats (Busk *et al.*, 2002). FSTL1 and S100A4 are secreted proteins that have been implicated in cancer cell growth.

Table 2. Echocardiography

	Weeks	n	AWTd	AWTs	PWTd	PWTs	LVD	LVAS	FAC
Aortic banding	6	6	0.237 ± 0.017*	0.434 ± 0.025*	0.247 ± 0.014*	0.426 ± 0.022*	0.495 ± 0.034	0.092 ± 0.015	0.820 ± 0.016
Sham	6	6	0.160 ± 0.004	0.318 ± 0.006	0.150 ± 0.003	0.313 ± 0.010	0.513 ± 0.021	0.105 ± 0.011	0.798 ± 0.016
Aortic banding	12	6	0.252 ± 0.008*	0.430 ± 0.016*	0.250 ± 0.007*	0.432 ± 0.011*	0.513 ± 0.026	0.115 ± 0.022	0.779 ± 0.037
Sham	12	6	0.155 ± 0.008	0.325 ± 0.016	0.152 ± 0.009	0.320 ± 0.011	0.480 ± 0.033	0.090 ± 0.024	0.822 ± 0.033
Aortic banding	16	8	0.270 ± 0.009*	0.448 ± 0.019*	0.264 ± 0.009*	0.444 ± 0.017*	0.499 ± 0.037	0.125 ± 0.026	0.757 ± 0.041
Sham	16	6	0.168 ± 0.007	0.330 ± 0.011	0.172 ± 0.007	0.330 ± 0.011	0.428 ± 0.027	0.092 ± 0.015	0.789 ± 0.028
Aortic banding	30	8	0.290 ± 0.017*	0.449 ± 0.018*	0.285 ± 0.015*	0.449 ± 0.021*	0.555 ± 0.043	0.188 ± 0.056	0.697 ± 0.068
Sham	30	6	0.195 ± 0.006	0.332 ± 0.008	0.178 ± 0.007	0.320 ± 0.010	0.513 ± 0.014	0.113 ± 0.015	0.778 ± 0.031
MI	3	17	0.097 ± 0.007*	0.101 ± 0.006*	0.176 ± 0.008	0.251 ± 0.006*	0.826 ± 0.027*	0.596 ± 0.025*	0.280 ± 0.015*
Sham	3	6	0.172 ± 0.005	0.303 ± 0.012	0.157 ± 0.006	0.303 ± 0.015	0.438 ± 0.029	0.108 ± 0.014	0.756 ± 0.021
MI	9	14	0.089 ± 0.007*	0.096 ± 0.013*	0.167 ± 0.007	0.241 ± 0.015*	0.975 ± 0.04*	0.756 ± 0.039*	0.222 ± 0.030*
Sham	9	6	0.163 ± 0.007	0.343 ± 0.007	0.160 ± 0.003	0.347 ± 0.007	0.503 ± 0.018	0.095 ± 0.007	0.812 ± 0.009
Shunt	3	10	0.168 ± 0.007	0.306 ± 0.015	0.172 ± 0.006*	0.314 ± 0.012*	0.618 ± 0.038*	0.206 ± 0.024*	0.673 ± 0.023*
Sham	3	6	0.152 ± 0.004	0.293 ± 0.011	0.148 ± 0.008	0.275 ± 0.008	0.418 ± 0.015	0.105 ± 0.011	0.751 ± 0.019
Shunt	8	12	0.160 ± 0.006	0.300 ± 0.013	0.159 ± 0.005	0.295 ± 0.011	0.825 ± 0.033*	0.295 ± 0.019*	0.639 ± 0.025
Sham	8	6	0.165 ± 0.002	0.308 ± 0.014	0.163 ± 0.006	0.303 ± 0.012	0.545 ± 0.026	0.148 ± 0.022	0.729 ± 0.040

Values are listed as mean ± SEM. Left ventricular anterior wall thickness (AWT), left ventricular posterior wall thickness (PWT), and left ventricular area (LVA) were measured by echocardiography in a short axis 2D view. Measurements were made in both systole (-s) and diastole (-d). Fractional area of change (FAC) was calculated as (LVA-d - LVA-s)/LVA-d and fractional shortening as (LVD-d - LVD-s)/LVD-d. * $p < 0.05$ vs. sham.

Table 3. The 139 known genes with common regulation in all hypertrophy models. Some genes are present in more than one category, but not all categories have been listed of each gene. See Supplemental Table A for a full list of genes by general functional category and detailed annotations

Category	Genes
Signal transduction	<i>Annexin-V</i> , scavenger receptor-B2, <i>KCNE1</i> , peptidylglycine α -amidating monooxygenase, <i>S100A10</i> , protein phosphatase-1a, protein kinase inhibitor- α , annexin-II, <i>CNP</i> , <i>Sult1a1</i> , <i>Gata4</i> , <i>TSC22</i> , <i>PDE4a</i> , <i>YWVK-II</i> , <i>FKBP1a</i> , dynein, <i>SMARCB1</i> , <i>NPPB</i> , <i>CD151</i> , phosphatidylinositol transfer protein- β , <i>MaoA</i> , annexin-I, protein phosphatase-1b, prostaglandin receptorF2- α , <i>Lsamp</i> , <i>NPPA</i> , <i>APP</i> , <i>granulin</i> , <i>CD9</i> , <i>KCNH2</i> , <i>MCP1</i> , <i>Slc3a2</i> , <i>PTPRO</i> , osteoprotegerin, <i>RNF28</i> , integrin- β 1, <i>UNC-119</i> , myoinositol monophosphatase-2
Cell growth/proliferation	<i>NdrG4</i> , annexin-V, <i>Btg1</i> , <i>GADD45A</i> , <i>Hsp27</i> , <i>TIMP1</i> , <i>FSTL1</i> , cyclin-D2, ribosomal protein-L6, <i>EGLN3</i> , <i>CSRP2</i> , <i>S100A4</i> , ribosomal protein-S27, ribosomal protein-L3, <i>granulin</i> , cyclin-D1, <i>Slc3a2</i> , <i>AIF1</i>
Cell death/apoptosis	Death-associated kinase-3, <i>GADD45A</i> , <i>Mfge8</i> , <i>EGLN3</i> , biglycan, fibronectin, <i>S100A4</i> , <i>APP</i> , <i>PRG1</i> , <i>Hsp40</i> homologue-A4, osteoprotegerin, <i>DNAJB5</i>
Development	<i>NdrG4</i> , vesicle-associated membrane protein-5, annexin-II, <i>Gata4</i> , osteopontin, <i>transgelin</i> , <i>EGLN3</i> , <i>Lsamp</i> , <i>CSRP2</i> , <i>S100A4</i> , <i>PRG1</i> , <i>MCP1</i> , <i>Integrin-β1</i> , <i>tropomyosin-4</i>
Defense/inflammation	<i>Gpx3</i> , <i>CD1D</i> , <i>Psmel</i> , osteopontin, <i>Hsp27</i> , complement C1-inhibitor, <i>Thy1</i> , <i>Lysozyme</i> , <i>Hsp90A</i> , annexin-I, <i>FCGRT</i> , <i>KLRG1</i> , <i>MCP1</i> , <i>AIF1</i> , <i>Pai1</i> , complement C1qb, <i>cathepsin-S</i> , <i>Fcgr3</i>
Cytoskeletal/ecm organisation	Protease nexin-1, <i>ARGBP2</i> , Actin- α skeletal muscle, tubulin- α 1, <i>CNP</i> , osteopontin, procollagen type 3- α 1, <i>transgelin</i> , <i>Hsp27</i> , α -actin, <i>TIMP1</i> , <i>cathepsin-L</i> , <i>profilin-1</i> , <i>TIMP2</i> , <i>MYL6</i> , <i>MYL9</i> , biglycan, <i>RLC</i> , fibronectin, α -actin vascular smooth muscle, vimentin, thrombospondin-4, lysyl oxidase, osteoprotegerin, sarcosin, <i>tropomyosin-4</i> , <i>Pai1</i> , <i>cathepsin-S</i>
Metabolism	<i>AQP7</i> , aldehyde dehydrogenase-1a1, <i>Pcyt2</i> , 4-hydroxyphenylpyruvate dioxygenase, <i>ACAT1</i> , 2,4-dienoyl-CoA reductase, dodecenoyl-CoA- Δ -isomerase, <i>Slc25a5</i> , <i>OSCP</i> , trifunctional protein- α , trifunctional protein- β , <i>PS-PLa1</i> , <i>GOT1</i> , <i>Sult1a1</i> , <i>GOT2</i> , retinol-binding protein-1, <i>CK-B</i> , ornithine decarboxylase antizyme inhibitor, <i>FACL2</i> , <i>Slc16a1</i> , <i>cathepsin-L</i> , ferritin light chain, <i>GNPAT</i> , glycogen phosphorylase, <i>SDHA</i> , guanylate kinase 1, <i>NNT</i> , natriuretic peptide receptor-3, <i>MaoA</i> , enoyl-CoA hydratase-like, phosphofructokinase-muscle, <i>ERp29</i> , <i>BCAT2</i> , succinyl-CoA ligase, <i>ACAA2</i> , <i>FUCA1</i> , Carbonic anhydrase-2, <i>CK-mit</i> , <i>COX8h</i> , <i>DLAT</i> , <i>ETFA</i> , <i>PDHA2</i> , <i>Slc7a1</i> , <i>AMA-CR</i> , <i>cathepsin-S</i> , <i>GAMT</i>
Unknown	<i>Nuclear receptor binding factor-1</i> , <i>ICT1</i> , major vault protein

Differences in gene expression patterns between hypertrophic phenotypes

We next looked for the transcriptional responses specific to each hypertrophy model by asking which genes showed expression differences between the different hypertrophic models, using ANOVA. This analysis identified 44 genes with differential expression between the models (Supplemental Table B). The genes represented 40 known genes, two ESTs and two replicates of ANP. Of these genes, 15 differed only in fold change between the models but were consistently either up- or downregulated in all models compared to controls (Supplemental Table B). A hierarchic cluster analysis of the 44 genes showed tight clustering of the disease models but separate clustering of the pharmacologically treated animals (Supplemental Figure A). Thus, the differences between the models primarily resulted from differences between the disease models and the pharmacologically treated animals. After exclusion of the pharmacologically treated animals, only seven genes were differentially expressed: *Mapk7*, skeletal α -actin, *Csrp2*,

acetyl-CoA acyltransferase, ANP (two genes) and an EST.

Confirmation by real-time PCR

To independently confirm the microarray data, mRNA levels of eight genes were analysed by real-time PCR (Figure 1). The real-time PCR analyses all confirmed the microarray findings, although the fold change tended to be greater when determined by real-time PCR.

Discussion

Our work addresses global aspects of gene regulation in surgical and pharmacological models of cardiac hypertrophy in mammals. Is there a common set of genes that largely defines cardiac hypertrophy in these models? To address this question, we compared transcriptome responses among five models of cardiac hypertrophy. We identified a set of 139 genes and 13 ESTs that were commonly regulated in cardiac hypertrophy in response to diverse

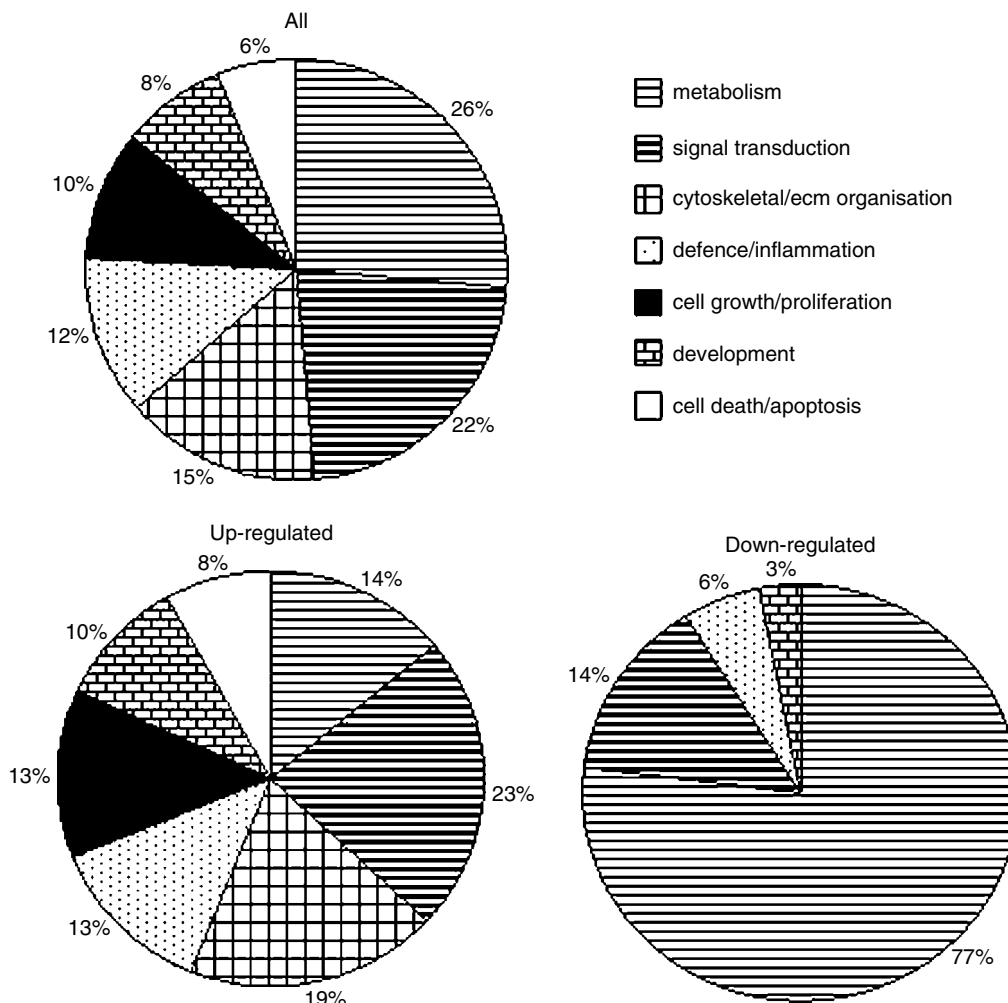


Figure 3. Known genes ($n = 139$) with common expression in all hypertrophic models were categorized based on function, as determined from database searches. Genes involved in the cytoskeleton/extracellular matrix (ecm) organization, cell death/apoptosis, and cell growth/proliferation were exclusively upregulated. The vast majority of downregulated genes were involved in the β -oxidation of fatty acids

and naturally occurring pathological stimuli, such as pressure overload, volume overload and myocardial infarction. Overall, this outcome is important for two reasons. First, these transcriptome changes are likely to signify molecular events necessary for, or a consequence of, the hypertrophic process in these models. Second, using a global approach, our data support and expand the notion of a universal gene program underlying cardiac hypertrophy in response to multiple diversified stimuli. This paradigm was previously based on transcriptional changes in a small set of genes, including immediate early genes, ANP, BNP, and sarcomer

genes constituting the so-called 'fetal gene program' (Chien *et al.*, 1991).

Many genes in our core set including ANP, BNP, β -actin, procollagen, fibronectin, GATA4, ribosomal proteins, biglycan, vimentin, Hsp27, TSC22, PAI1, and osteopontin were consistently regulated in previous microarray studies analyzing the myocardium after MI in rats, in failing hearts from hypertensive rats, in neonatal and adult mice and in failing and hypertrophic human hearts (Supplemental table A) (Anversa *et al.*, 1983; Barrans *et al.*, 2002; Friddle *et al.*, 2000; Hwang *et al.*, 2000, 2002; Schoenfeld *et al.*, 1998; Sehl *et al.*,

2000; Stanton *et al.*, 2000; Yang *et al.*, 2000). Remarkably, although these studies employed different experimental setups and microarray technologies, including self-made or customized arrays containing cDNAs or oligonucleotides, and different clustering algorithms, they reported many similar transcriptome changes, of which the most highlighted were upregulation of ecm proteins (Anversa *et al.*, 1983; Barrans *et al.*, 2002; Friddle *et al.*, 2000; Hwang *et al.*, 2000, 2002; Schoenfeld *et al.*, 1998; Sehl *et al.*, 2000; Stanton *et al.*, 2000; Yang *et al.*, 2000). Employing two hormone-induced hypertrophy models in mice, Friddle *et al.* (2000) found 38 annotated gene changes, of which 16 was included in our common hypertrophy genes. Using Affymetrix arrays, Weinberg *et al.* (2003) reported increased expression of a number of genes in response to acute and chronic pressure overload in male and female mice. Of 12 483 tested genes, 68 genes were upregulated in males and females, of which several were consistent with our results, including ornithine decarboxylase antizyme inhibitor, fibronectin, tissue-inhibitor of metalloproteinase, procollagen, glutathione peroxidase 3, nexin, thrombospondin, biglycan, skeletal α -actin, β -actin and ANP. However, to the best of our knowledge no other study compares transcriptome changes across the multiple forms of hypertrophy we here employed. Furthermore, the large sample set ($n = 46$) allowed us to use the Bonferroni correction that reduces the amount of false positives.

We employed diverse pathological stimuli to induce hypertrophy in the animals, but only a few genes were differentially expressed between the models (44 genes). The transcriptome differences between models were primarily between the surgical models and the hormone-stimulated models, which could be due to the selective nature of hormone stimulation as compared to more complex stimuli in the surgical models. Perhaps predictably, hormone infusion might be less suited for determination of genes regulated by pathophysiological processes *in vivo* than actual disease models.

Although these findings indicate that overall the gene expression in the different surgical models is more similar than different, it should be taken into consideration that this study was designed primarily to identify a common trunk of genes across models. The statistical power declines when subgrouping samples, resulting in an increased risk of type 2 errors, i.e. missing genes that actually

change. In addition, we used a conservative statistical correction (Bonferroni) to keep type 1 statistical error (false positives) low despite the multiple comparisons ($\alpha_{\text{total}} < 0.05$). Had we used a less stringent statistical approach, we could have found a higher number of transcriptome changes between the models.

Our data suggest that the essential attributes of hypertrophic remodelling of the myocardium include:

1. *Activation of growth-inducing molecules*, including enhanced expression of growth factors (Mcp, S100A4, Mgfe8 and granulin, both EGF-like proteins), cyclin D2, FSTL1 (growth factor implicated in cancer), TGF β signalling proteins, and several ribosomal proteins.
2. *Activation of multiple signalling modules*, including those leading to: (a) accumulation of inositol phosphates (enhanced expression of receptors that stimulate PI accumulation), PI transfer protein-B (engaged in phospholipid transport), CD9 and CD151 (link PKC to specific integrins), and myoinositol monophosphatase, and (b) changes in Ca²⁺ handling, ion-channels (KCNE1 and KCNH2) and channel-associated proteins, dubbed annexins.
3. *Enhanced remodelling through ecm and cytoskeletal systems*, including cytoskeletal-associated proteins, such as myosin and dynein (cytoskeletal molecular motors), vimentin, SMAR-CH1 β (an actin-dependent regulator of chromatin remodelling), fibronectin, ecm proteases, transgelin (participates in cytoskeleton assembly), ArgBP2 (a Src-3 domain containing protein that binds to sarcomer elements) and integrin are enhanced.
4. *Engagement of defence and inflammation proteins related to coagulation and lymphocyte activation* were enhanced, such as annexins, protease nexin-1, pai-1, complement C1 inhibitor, and complement C1gb).
5. *Changes in genes involved in energy metabolism* suggest a shift away from lipids as the main energy source in the myocardium, consistent with previous reports (Stanton *et al.*, 2000; Yang *et al.*, 2000). Several key regulatory genes involved in fatty acid oxidation pathways, e.g. acetyl-CoA acyltransferase, dienoyl CoA-reductase, fatty acid CoA-ligase, dodecenoyl CoA-isomerase, and enoyl CoA-hydratase were

repressed, as depicted in Supplemental Figure B. Many genes involved in the mitochondrial respiratory chain, e.g. OSCP, SDHA, NNT, COX8h and ETFA, were downregulated, indicating a general defect in energy metabolism in hypertrophic hearts, as also noted by others (Stanton *et al.*, 2000; Yang *et al.*, 2000).

A notable finding was that upregulation of three annexins (I, II and V), members of a family of proteins that have anticoagulant effects, inhibits leukocyte infiltration, and form Ca²⁺ channels. Annexin upregulation might have beneficial effects. Annexin I peptides protect against ischaemia-reperfusion injury of the myocardium, most likely by inhibiting leukocyte infiltration (La *et al.*, 2001). Annexin channel formation might be required for changes in Ca²⁺ homeostasis and gene expression in hypertrophic cardiomyocytes. In hypertrophic chondrocytes, annexin-mediated Ca²⁺ influx activates gene expression of Cbfa1, ATPase and osteocalcin, which are differentiation markers in these cells (Wang *et al.*, 2003).

Another interesting finding was increased expression of granulin, a growth factor that resembles the EGF/TGF α family, although granulin does not activate EGF receptors (Bateman *et al.*, 1998). Granulins regulate differentiation/proliferation of multiple cells, including epithelial and haematopoietic cells and carcinoma and breast cancer cell lines. Granulin was found upregulated in human glioblastomas in a cDNA microarray study (Liau *et al.*, 2000). Further work will reveal whether granulin plays a role in cardiomyocyte hypertrophy. It should be noted that TSC-22 (TGF β -controlled transcription factor), FSTL1, and PAI-1 (TGF β -induced effectors) were upregulated, suggesting that activation of TGF β family signalling is involved in hypertrophy, as also noted by others (Stanton *et al.*, 2000).

In conclusion, we have identified a set of genes common to several different clinically relevant phenotypes of cardiac hypertrophy. These genes are likely to be central to hypertrophic phenotype, irrespective of the initiating cause.

Acknowledgements

We thank Paul C. Simpson, UCSF, for critical reading of the manuscript, and Bettina Collin, Pernille Gundelach, Tordis Christiansen and Katrine Kastberg for technical assistance. The work was supported by the John and Birthe Meyer

Foundation; The Danish Heart Foundation (Grant Nos 01-1-2-59-22907, 99-1-2-31-22684); The Villadsen Family Foundation; The Foundation of 17.12.1981, University of Copenhagen, Rigshospitalet; and the Danish National Research Foundation.

References

- Agabiti-Rosei E, Muiesan ML. 1997. Prognostic significance of left ventricular hypertrophy regression. *Adv Exp Med Biol* **432**: 199–205.
- Anversa P, Levicky V, Beghi C, McDonald SL, Kikkawa Y. 1983. Morphometry of exercise-induced right ventricular hypertrophy in the rat. *Circ Res* **52**: 57–64.
- Aronow BJ, Toyokawa T, Canning A, *et al.* 2001. Divergent transcriptional responses to independent genetic causes of cardiac hypertrophy. *Physiol Genom* **6**: 19–28.
- Barrans JD, Allen PD, Stamatou D, Dzau VJ, Liew CC. 2002. Global gene expression profiling of end-stage dilated cardiomyopathy using a human cardiovascular-based cDNA microarray. *Am J Pathol* **160**: 2035–2043.
- Bateman A, Bennett HJP. 1998. Granulins: the structure and function of a emerginc family of growth factors. *J Endocrinol* **158**: 145–151.
- Busk PK, Bartkova J, Strom CC, *et al.* 2002. Involvement of cyclin D activity in left ventricle hypertrophy *in vivo* and *in vitro*. *Cardiovasc Res* **56**: 64–75.
- Chien KR, Knowlton KU, Zhu H, Chien S. 1991. Regulation of cardiac gene expression during myocardial growth and hypertrophy: molecular studies of an adaptive physiologic response. *FASEB J* **5**: 3037–3046.
- Fridde CJ, Koga T, Rubin EM, Bristow J. 2000. Expression profiling reveals distinct sets of genes altered during induction and regression of cardiac hypertrophy. *Proc Natl Acad Sci USA* **97**: 6745–6750.
- Golub TR, Slonim DK, Tamayo P, *et al.* 1999. Molecular classification of cancer: class discovery and class prediction by gene expression monitoring. *Science* **286**: 531–537.
- Hwang DM, Dempsey AA, Lee CY, Liew CC. 2000. Identification of differentially expressed genes in cardiac hypertrophy by analysis of expressed sequence tags. *Genomics* **66**: 1–14.
- Hwang JJ, Allen PD, Tseng GC, *et al.* 2002. Microarray gene expression profiles in dilated and hypertrophic cardiomyopathic end-stage heart failure. *Physiol Genom* **10**: 31–44.
- La M, D'Amico M, Bandiera S, *et al.* 2001. Annexin 1 peptides protect against experimental myocardial ischemia-reperfusion: analysis of their mechanism of action. *FASEB J* **15**: 2247–2256.
- Li C, Hung Wong W. 2001a. Model-based analysis of oligonucleotide arrays: model validation, design issues and standard error application. *Genome Biol* **2**.
- Li C, Wong WH. 2001b. Model-based analysis of oligonucleotide arrays: expression index computation and outlier detection. *Proc Natl Acad Sci USA* **98**: 31–36.
- Liau LM, Lallone RL, Seitz RS, *et al.* 2000. Identification of a human glioma-associated growth factor gene, granulin, using differential immunoadsorption. *Cancer Res* **60**: 1353–1360.
- Roberts CJ, Nelson B, Marton MJ, *et al.* 2000. Signalling and circuitry of multiple MAPK pathways revealed by a matrix of global gene expression profiles. *Science* **287**: 873–880.

- Schoenfeld JR, Vasser M, Jhurani P, et al. 1998. Distinct molecular phenotypes in murine cardiac muscle development, growth, and hypertrophy. *J Mol Cell Cardiol* **30**: 2269–2280.
- Sehl PD, Tai JT, Hillan KJ, et al. 2000. Application of cDNA microarrays in determining molecular phenotype in cardiac growth, development, and response to injury. *Circulation* **101**: 1990–1999.
- Stanton LW, Garrard LJ, Damm D, et al. 2000. Altered patterns of gene expression in response to myocardial infarction. *Circ Res* **86**: 939–945.
- Wang W, Xu J, Kirsch T. 2003. Annexin-mediated Ca^{2+} influx regulates growth plate chondrocyte maturation and apoptosis. *J Biol Chem* **278**: 3762–3769.
- Weinberg EO, Mirotso M, Gannon J, et al. 2003. Sex dependence and temporal dependence of the left ventricular genomic response to pressure overload. *Physiol Genom* **12**: 113–127.
- Wollert KC, Taga T, Saito M, et al. 1996. Cardiotrophin-1 activates a distinct form of cardiac muscle cell hypertrophy. Assembly of sarcomeric units in series VIA gp130/leukemia inhibitory factor receptor-dependent pathways. *J Biol Chem* **271**: 9535–9545.
- Yang J, Moravec CS, Sussman MA, et al. 2000. Decreased SLIM1 expression and increased gelsolin expression in failing human hearts measured by high-density oligonucleotide arrays. *Circulation* **102**: 3046–3052.